Properties of Spanning Water Networks at Protein Surfaces

Nikolai Smolin, Alla Oleinikova, Ivan Brovchenko,* Alfons Geiger, and Roland Winter

Physikalische Chemie, Universität Dortmund, Otto-Hahn-Strasse 6, Dortmund, D-44227, Germany

Received: January 10, 2005; In Final Form: March 21, 2005

The formation of a spanning two-dimensional hydrogen-bonded water network at the surface of proteins via a percolation transition enables their biological function. We show in detail how the spanning (percolating) water network appears at the surfaces of model hydrophilic spheres and at the surface of a single protein (lysozyme) molecule. We have found essential correlations of the linear extension, radius of gyration, and position of the center of mass of the largest water cluster with its size. The specific two-peak structure of the probability distribution of the largest cluster size allowed us to study various properties separately for spanning and nonspanning largest clusters. The radius of gyration of the spanning cluster always exceeds the radii of the spheres or the effective radius of the protein. Any spanning cluster envelops essentially more than half of the surface area. The temporal decay of the spanning networks shows a stretched exponential character. Their average lifetime at the percolation threshold is about the lifetime of a water−water hydrogen bond.

1. Introduction

Hydration water plays an important role in protein functions.[1−3] Local and orientational ordering of water molecules near hydrophobic and hydrophilic parts of protein surfaces were extensively studied during past decades both experimentally[3−8] and by computer simulations (see, for example, refs 9−12). Dynamic properties of water are strongly affected by the protein surface, and their changes are sensitive to the particular chemical structure of the protein.[13−18] Structural and dynamic properties of proteins depend on the hydration level.[19−24] In particular, about one "monolayer" of water is required for restoring the full internal dynamics of proteins and their function.[1−3]

Experimental studies on protein powders indicate the onset of some biological functions only when an infinite water network spans the protein surface.[2,25−29] It is generally accepted that enzymes require internal flexibility for their biological activity, but what kind of motions are required is not yet clear.[30] There seems to be no direct correlation between the enzymatic activity and the global dynamics of proteins.[31] However, the biological activity of proteins could be driven by the dynamics of hydration water.[32] In fact, the effect of solvent fluctuations (in the enthalpy, volume, and dipole moment) on proteins may be of fundamental importance, as fluctuations permit conformational motions. These motions may be "slaved" or they may be "nonslaved" in the case of the protein motions being independent of solvent fluctuations.[33] Slaved motions therefore have rates that are proportional to the fluctuation rate of the solvent. In a recent study on myoglobin,[33] it has been found that the activation enthalpy of protein conformational and vibrational dynamics is controlled by the activation enthalpy of the solvent. Hence, the fluctuations in the amino acid residues and their hydration shells are coupled to and dominated by the surrounding solvent thermal bath. On the contrary, the protein and its hydration shell control the activation entropy through the shape of the energy landscape.[33] The prevalence of slaved motions, such as the opening and closing of channels, ligand binding, and enzyme catalysis, highlights the importance of the solvational environment of cells for the function of proteins.

Because the onset of enzymatic activity coincides with the formation of an infinite (spanning) network of hydration water via a two-dimensional (2D) percolation transition,[2] a qualitative change of some dynamic properties of the hydrated protein should be expected at the percolation threshold. Recently, we studied the 2D percolation transition of hydration water by computer simulations.[34] It was found that the formation of a spanning water network at the surface of a single protein molecule occurs in a similar way as to that in a protein powder. A collective infinite water network in protein powder appears at a low hydration level and covers less than half of the hydrophilic surface of each protein molecule. This means that the first appearance of biological activity may not ultimately need the existence of a *spanning* network around a single protein molecule but rather the existence of a water network connecting some particular sites of one or several proteins. Comparison of the simulated hydration process[34] with experimental observations[2] indicates that the formation of an individual fractal-like percolating water network, which envelops each protein molecule, can be identified with the first appearance of a water "monolayer", which restores the full internal dynamics of the protein.

To clarify the role of water in the appearance of biological function of proteins, the study of structural and dynamic properties of proteins should be carried out with respect to the formation of collective as well as individual spanning water networks. This study should be accompanied by the comparison of various properties of the hydration water networks above and below the percolation threshold. The specific properties of a spanning network of hydration water have not been studied yet, contrary to the various properties of local water networks.[3−12]

Simulations of hydrated protein powders are possible nowadays within crude models only (see ref 34 for a detailed discussion of this problem), making it impossible to study dynamic properties as well. However, the structure and dynamics of a single hydrated protein molecule and its hydration water can be studied by modern computer simulation methods, both

* Author to whom correspondence should be addressed. E-mail: brov@heineken.chemie.uni-dortmund.de

10.1021/jp050153e CCC: $30.25
Published on Web 05/11/2005

at low hydration levels and in aqueous solution. This should be done with and without the presence of a spanning network of hydration water, i.e., under conditions above and below the percolation threshold. Hence, location of the spanning network of hydration water is a necessary prerequisite of such studies.

In view of the complexity of the protein−water system, it is reasonable to study a spanning water network first for a rigid model protein. Such an approach neglects conformational changes of the protein molecule upon hydration. These changes can noticeably affect topological and chemical properties of the surface and its area accessible for water molecules and may shift the percolation threshold. However, the main properties of a spanning water network and the regularities of its formation are expected to be rather universal and, therefore, should be similar for rigid and flexible models of proteins.

It is not obvious how to distinguish spanning and nonspanning networks at the surface of a finite object. Recently, we have shown that conventional methods of analysis of clustering and percolation can be used to locate a percolation transition of water at the surface of a hydrophilic sphere or protein (lysozyme) molecule.[34] In the present paper, we studied various topological and dynamic properties of spanning and nonspanning water networks in such systems as a function of the level of hydration, temperature, and object size. Moreover, we propose several criteria how to detect in simulations the existence of a spanning network at the surface of a finite object.

2. Methods

Molecular dynamics (MD) simulations of lysozyme + water systems were carried out in an *NVT* ensemble, using a rigid model of lysozyme with the crystallographic heavy atom coordinates from ref 35, the force field from ref 36, and the TIP4P water model.[37] Trajectories from 8 to 15 ns were used to analyze water clustering and properties of the largest cluster at various hydration levels every hundredth integration step (every 0.2 and 0.1 ps at $T = 300$ and 400 K, respectively). Such properties were also studied for water at the surfaces of the smooth hydrophilic spheres with radii $R_{sp} = 15$, 30, and 50 Å by Monte Carlo (MC) simulations in the *NVT* ensemble. The water−surface interaction was modeled by a (9−3) Lennard-Jones potential with $\sigma = 2.5$ Å and well depth $U_0 = -19.34$ kJ/mol. Configurations after every 1000 MC steps were analyzed, providing up to 5×10^5 analyzed configurations for each hydration level. Details of the simulations can be found elsewhere.[34]

The occurrence of a 2D liquid−vapor phase transition could distort or even prevent the surface percolation transition. To avoid 2D condensation (layering transition), simulations of water at the surface of hydrophilic spheres were performed at $T = 425$ K, which exceeds the critical temperature of the layering transition ($T \approx 400$ K) for the studied water−surface interaction strength.[38] Simulations of hydrated lysozyme molecules were performed at 300 and 400 K to explore the effect of temperature on the simulated properties. The lower temperature is of practical importance and allows comparison with experimental data, whereas the higher temperature was chosen to be able to compare water clustering at the surface of lysozyme with that at the smooth hydrophilic spherical surfaces.

The various hydration levels were obtained by adding N_w water molecules to the simulation box, which varies from $N_w = 200$ to 600 at $T = 300$ K and from 400 to 800 at $T = 400$ K in the case of the lysozyme molecule. N_w varies from 150 to 450 for the sphere of radius $R_{sp} = 15$ Å, from 900 to 1300 for $R_{sp} = 30$ Å, and from 2500 to 3400 for $R_{sp} = 50$ Å. The hydration level was also characterized by the surface coverage C. For a spherical surface, $C = N_w/4\pi(R_{sp} + 3\ \text{Å})^2$, where 3 Å is the distance from the considered hydrophilic surface to the first maximum of the oxygen local density.[38] The surface coverage of the single lysozyme molecule was estimated as $C = N_w/\text{SASA}$, were SASA is the solvent accessible surface area, found to be about 6900 Å^2.[34]

Water molecules are considered to belong to the same cluster if they are connected by a continuous hydrogen-bonded network. Two water molecules were considered as hydrogen bonded when the distance between the oxygen atoms is less than 3.5 Å and the water−water pair interaction energy is less than −10.0 kJ/mol.

Several properties of the largest clusters S_{max} were studied at various hydration levels. The size distribution of the largest clusters $P(S_{max})$, studied in our previous paper,[34] allows us to distinguish the spanning and nonspanning largest clusters. The linear extension of the largest cluster is characterized by the maximum distance L_{max} between two oxygens of water molecules in the largest cluster. The compactness of the largest clusters could be measured by the radius of gyration R_g

$$R_g = \sqrt{\sum_{i=1}^{N} m_i(\vec{\mathbf{r}}_i - \vec{\mathbf{r}}_0)^2 / \sum_{i=1}^{N} m_i} \qquad (1)$$

where m_i is the mass of water molecule and $\vec{\mathbf{r}}_i$ is a vector that defines the position of the ith water molecule relative to the center of a sphere or to the center of mass of lysozyme, whereas $\vec{\mathbf{r}}_i - \vec{\mathbf{r}}_0$ is its distance to the center of mass of the largest cluster located at $\vec{\mathbf{r}}_0 = \sum_i m_i \vec{\mathbf{r}}_i / \sum_i m_i$. The spanning properties of the largest cluster could also be described by the position of the center of mass of the largest cluster H_{max} relative to the center of mass of the sphere or the protein

$$H_{max} = \sqrt{\vec{\mathbf{r}}_0^{\,2}} \qquad (2)$$

The structure of the hydration water in a surface layer was described using oxygen−oxygen radial distribution functions $g_{O-O}(r)$ of water as a function of the hydration level. The lifetime of water hydrogen bonds and the spanning water network were also analyzed using conventional methods.[39]

3. Results

In a finite system (with periodic or open boundary conditions) and in a closed system without boundaries (such as the surface of a finite object), the percolation transition is smeared out. As a result, contrary to infinite systems, various properties of clusters indicate the percolation threshold at slightly different hydration levels. In particular, close to the percolation threshold, the probability distribution $P(S_{max})$ of the size S_{max} of the largest water cluster shows a pronounced two-peak structure. The small size peak of $P(S_{max})$ represents the nonspanning (finite) largest clusters, while the large size peak is due to spanning (infinite) clusters. When the two peaks are of comparable heights, the probability R to observe a spanning cluster is about 50%. At this hydration level (denoted as C_1), the mean cluster size S_{mean}, calculated excluding the largest cluster, approximately reaches its maximum. The fractal dimension d_f of the largest cluster achieves its 2D threshold value $d_f^{2D} \approx 1.896$ at the slightly higher hydration level C_2. Roughly at the same hydration level, the cluster size distribution n_S obeys the power law behavior $n_S \approx S^{-2.05}$ over the widest range of cluster sizes. The hydration level C_2 corresponds to the minimum water coverage, which

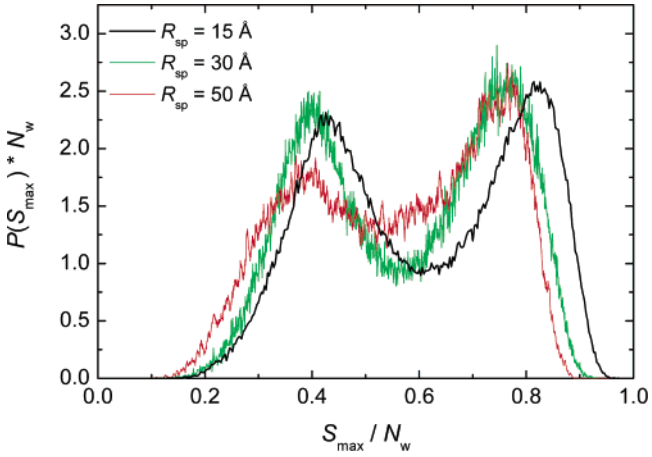

Figure 1. Probability distribution $P(S_{max})$ of the size S_{max} of the largest water cluster normalized to the total number of water molecules N_w on the surface of hydrophilic spheres with radii $R_{sp} = 15$, 30, and 50 Å at the hydration level C_1, where the probability to find a spanning water network is about 50%.

enables the persistent existence of a spanning water network at the surface. More details of the definitions of the hydration levels C_1 and C_2 can be found in our previous paper (ref 34).

It is reasonable to perform the comparison of various properties of spanning and nonspanning water networks at the hydration level C_1, where both kinds of the largest clusters exist with equal probability. This threshold hydration level was determined in our previous paper.[34] At $T = 425$ K, C_1 is about 0.086 Å^{-2} ($N_w \approx 350$), 0.088 Å^{-2} ($N_w \approx 1200$), and 0.087 Å^{-2} ($N_w \approx 3100$) for the studied hydrophilic spheres of radii 15, 30, and 50 Å, respectively. The threshold hydration level C_1 of a single lysozyme molecule was found to be about 0.058 Å^{-2} ($N_w \approx 400$) at $T = 300$ K and 0.091 Å^{-2} ($N_w \approx 625$) at $T = 400$ K. The probability distributions $P(S_{max})$ of size S_{max} of the largest water cluster on the surfaces of three hydrophilic spheres at the hydration level C_1 are compared in Figure 1. The two-peak structure of $P(S_{max})$ is caused by the finite size of the system and is expected to vanish with increasing surface area. However, Figure 1 shows that the two peaks are weakly sensitive to the surface area and remain pronounced and well-separated even at the surface of a very large sphere (radius $R_{sp} = 50$ Å) with a surface area of more than 35 000 Å^2. Taking into account that the two-peak structure of $P(S_{max})$ disappears at significantly smaller surface areas in the case of a planar surface with periodic boundary conditions,[40] we may conclude that the specific closed surface topology of spherical surfaces enhances such a two-peak structure. This effect also appears in the larger distance between the positions of the peaks of $P(S_{max})$ in the case of spherical surfaces in comparison with planar surfaces. Namely, in the latter case the average spanning cluster is about 1.6 times larger than the average nonspanning largest cluster,[40] whereas at the spherical surface this ratio is about 2.[34] Such peculiarity of a spherical surface allows a clear separation of the spanning and nonspanning networks, which is very useful for their comparative analysis, as we will see below. Examples of the arrangement of water molecules in the cases of the spanning and nonspanning largest water clusters on a spherical hydrophilic surface are shown in Figure 2.

The probability distributions of the maximum linear extension L_{max} of the largest water cluster $P(L_{max})$ are shown in Figure 3 as a function of L_{max}, normalized to the effective diameter of a hydrophilic sphere, $2(R_{sp} + 3$ Å), which accounts for the distance of about 3 Å from the surface to the location of the water oxygens in the first hydration layer. For clusters with all

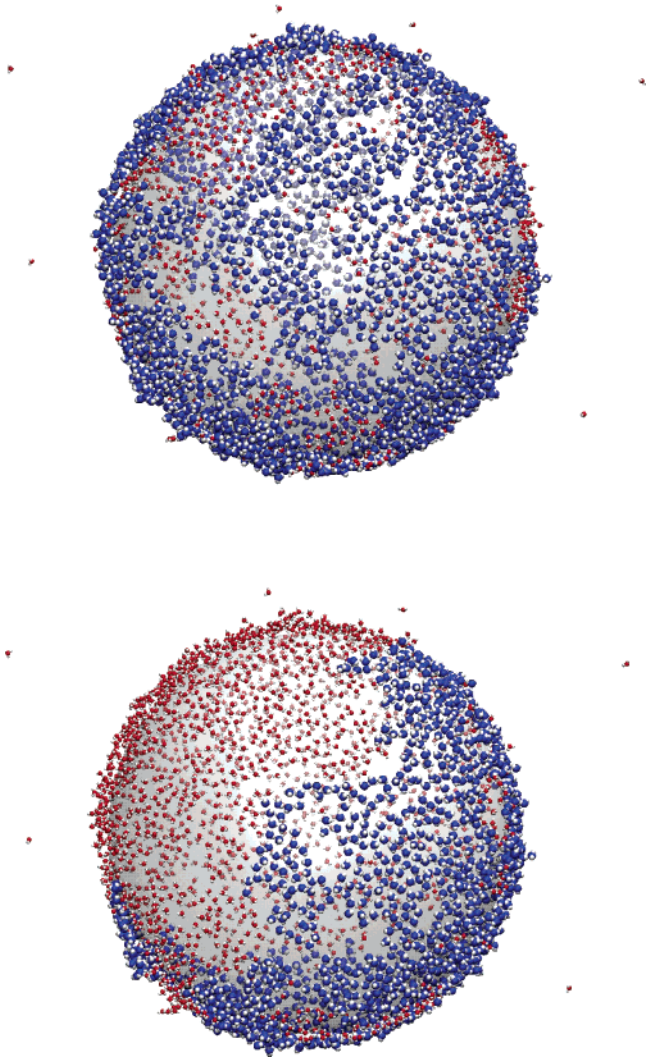

Figure 2. Arrangement of water molecules on the surface of a (transparent) hydrophilic sphere of radius $R_{sp} = 50$ Å at the hydration level C_1, where the probability to find a spanning water network is about 50% ($T = 425$ K, $N_w = 3100$). The oxygen atoms of the water molecules that belong to the largest cluster are colored in blue, those of all other water molecules in red. An example of a spanning and a nonspanning largest water cluster is shown in the upper and lower panel, respectively.

water molecules in the first hydration shell, the value of $L_{max}/2(R_{sp} + 3$ Å) does not exceed 1. Figure 3 shows that even at low hydration levels the largest clusters extend through the essential part of the spherical surface. The radial distribution function $g_{O-O}(r)$ of surface water at smooth hydrophilic surfaces shows a specific maximum at $r \approx 5.4$ Å, indicating the presence of chainlike water structures.[41] Due to such structure formation, the largest cluster is ramified, and even at low surface coverage ($C \approx 0.065$ Å^{-2}), its extension is comparable with the diameter of the sphere. At the surface coverage C_1, when the probability R to observe a spanning cluster is about 50%, for the vast majority of the largest clusters (both spanning and nonspanning), L_{max} exceeds $2(R_{sp} + 3$ Å) (the blue lines in Figure 3). At a larger surface coverage, L_{max} noticeably exceeds $2(R_{sp} + 3$ Å) because the largest cluster includes water molecules that do not belong to the first hydration shell.

To analyze the behavior of L_{max} separately for the spanning and nonspanning largest clusters, we have to classify each largest cluster of the size S_{max} using the two-peak structure of the distribution $P(S_{max})$. For this purpose, we calculated joint

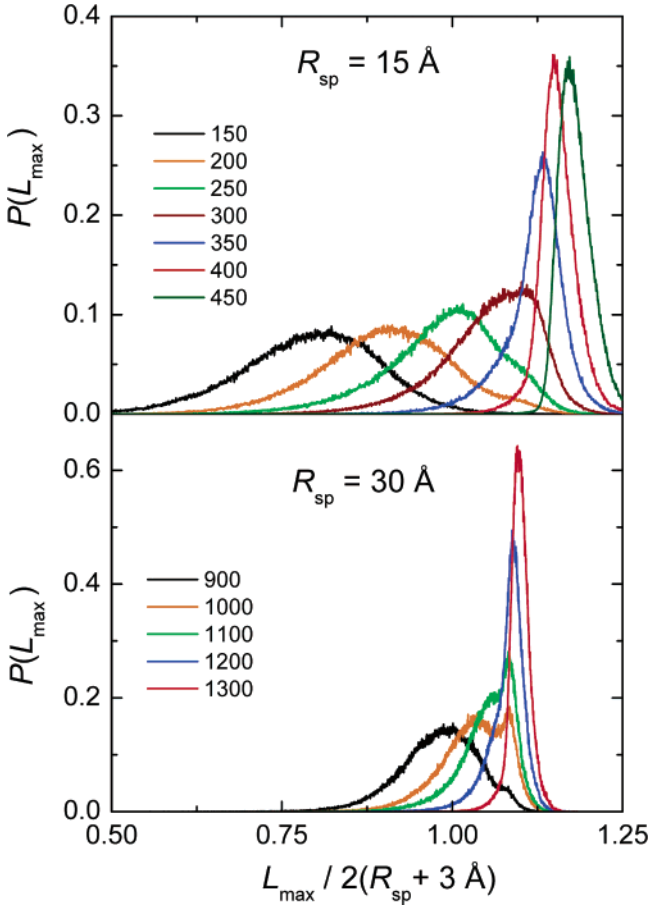

Figure 3. Probability distribution $P(L_{max})$ of the maximum linear extension L_{max} of the largest water cluster at the surface of two hydrophilic spheres (R_{sp} = 15 and 30 Å) at T = 425 K and various hydration levels N_w given in the inset. The blue and red lines approximately correspond to the surface coverages C_1 and C_2, respectively.

probability distributions $P(L_{max},S_{max})$ for various hydration levels. For the spherical surface with R_{sp} = 30 Å, $P(L_{max},S_{max})$ obtained at the threshold hydration level C_1 is shown in Figure 4. The two clearly separated peaks in $P(L_{max},S_{max})$ correspond to the spanning and nonspanning largest clusters. The projection of this probability distribution on the plane $L_{max}S_{max}$ is shown in the upper panel of Figure 5 (shading is proportional to the probability density). The two shadowed areas in Figure 5 (upper panel) correspond to the two peaks in Figure 4; the left-hand and right-hand areas represent the largest nonspanning and spanning water clusters, respectively. It is clearly seen from Figures 4 and 5 that these two peaks of $P(L_{max},S_{max})$ are hardly resolved, if considering the projection of $P(L_{max},S_{max})$ on the L_{max} axis. Indeed, the nonspanning largest clusters can be characterized by an average value of the maximum linear extension L_{max} of about 70 Å, whereas for the spanning clusters $L_{max} \approx 72$ Å (Figure 5, upper panel). These values correspond to $L_{max}/2(R_{sp} + 3\ \text{Å}) = 1.06$ and 1.09 for the largest nonspanning and spanning cluster, respectively, and they can be hardly distinguished as a faint shoulder in Figure 3 (lower panel, blue line). This difference becomes totally indistinguishable for smaller spheres (Figure 3, upper panel, blue line).

A similar analysis of the maximum extension L_{max} of the largest water cluster was performed for the hydrated lysozyme molecule. The evolution of the probability distribution $P(L_{max})$ with increasing hydration level is shown in Figure 6. Contrary to the spherical surface, the two maxima in $P(L_{max})$ can be seen

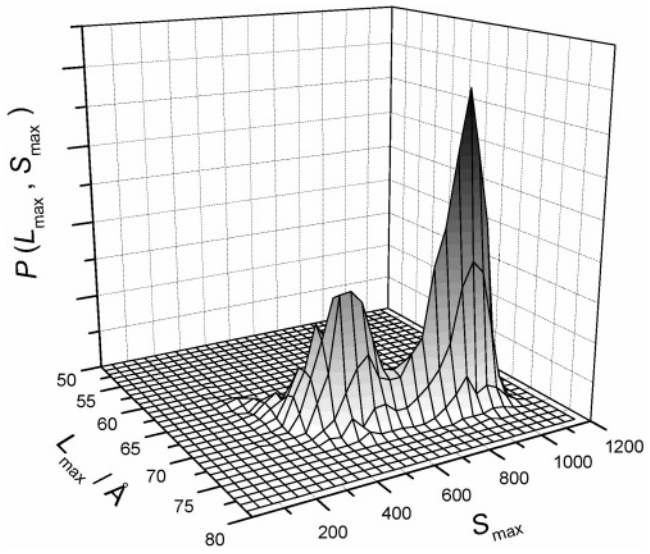

Figure 4. Joint probability distribution $P(L_{max},S_{max})$ of the maximum linear extension L_{max} and size S_{max} of the largest water cluster at the spherical surface of radius R_{sp} = 30 Å at T = 425 K and hydration level $C_1 \approx 0.088$ Å^{-2} (N_w = 1200).

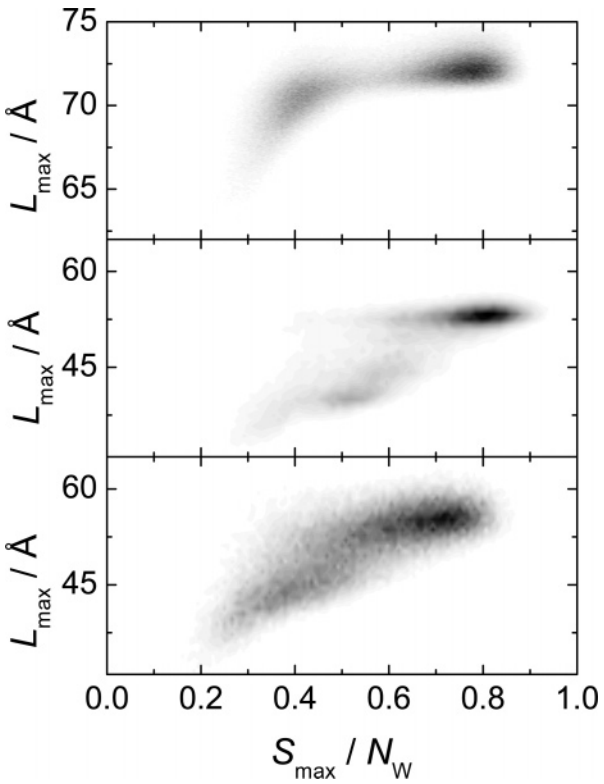

Figure 5. Projection of the joint probability distribution $P(L_{max},S_{max})$ of the linear extension L_{max} and size S_{max} of the largest water cluster at the surface of a hydrophilic sphere of R_{sp} = 30 Å (upper panel, N_w = 1200) at T = 425 K and on the surface of lysozyme at T = 300 K (middle panel, N_w = 400) and T = 400 K (lower panel, N_w = 625). The hydration level in all cases corresponds to the threshold hydration level C_1. Shading is proportional to probability density. Each panel has its own (proper) probability scale.

over a wide range of hydration. With an increase in temperature, $P(L_{max})$ becomes smoother, but the two maxima are still pronounced (Figure 6, lower panel). Similar to smooth surface, the radial distribution function $g_{O-O}(r)$ of water near the lysozyme surface shows a specific maximum at $r \approx 5.4$ Å, reflecting its chainlike structure over a wide range of hydration levels.

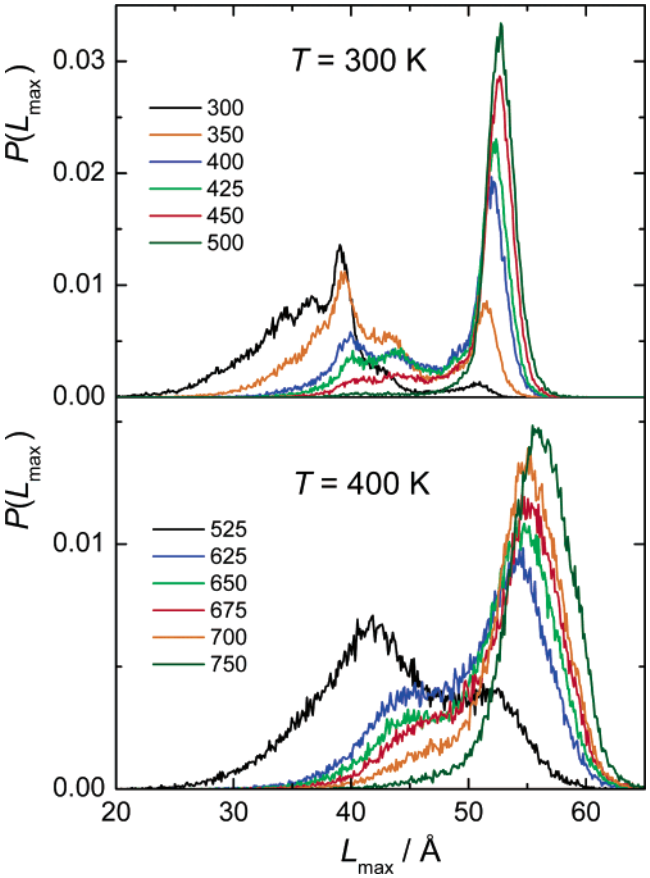

Figure 6. Probability distribution of the maximum linear extension L_{max} of the largest water cluster at the surface of lysozyme at two temperatures and various hydration levels. (N_w is given in the inset.) The blue and red lines approximately correspond to the threshold surface coverages C_1 and C_2, respectively.

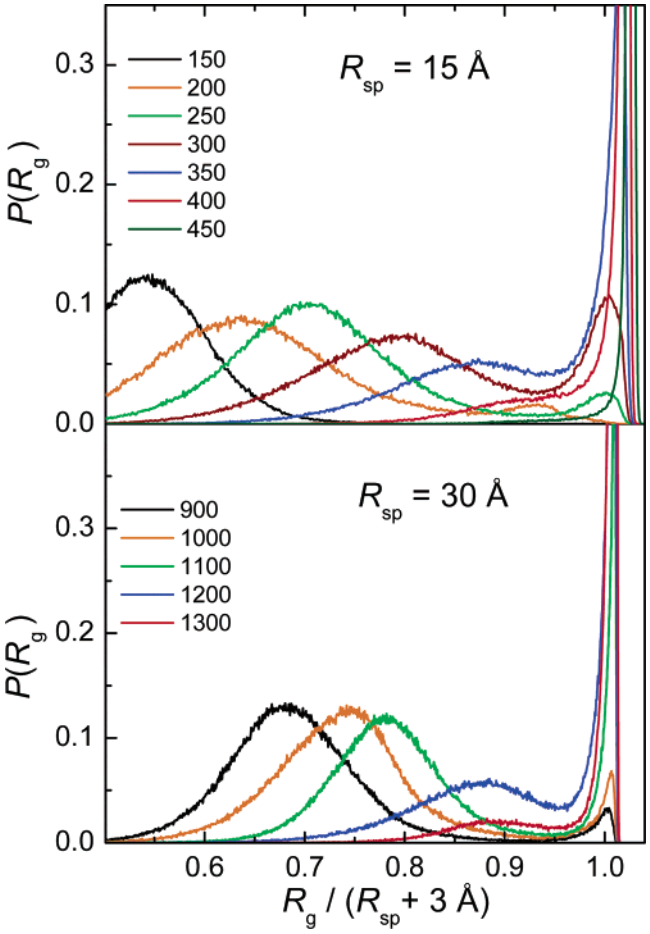

Figure 7. Probability distributions $P(R_g)$ of the radius of gyration R_g of the largest water cluster at the surfaces of two hydrophilic spheres of $R_{sp} = 15$ and 30 Å at $T = 425$ K and hydration levels N_w given in the inset. Blue and red lines approximately correspond to the surface coverages C_1 and C_2, respectively.

The projection of the joint probability distribution $P(L_{max},S_{max})$, calculated at the threshold hydration level C_1 for two temperatures, is shown in Figure 5. The two dark areas in both the middle and the lower panels in Figure 5 can be used to distinguish the spanning and nonspanning largest clusters at each temperature. Figures 5 and 6 indicate that the average maximum extension L_{max} of nonspanning clusters at the lysozyme surface is about 40 Å, whereas the average value of $L_{max} \approx 55$ Å can be attributed to spanning clusters.

The noticeable difference between the average values of L_{max} for spanning and nonspanning clusters on the lysozyme surface is obviously determined by the topology of the protein molecule. It could be due to the nonspherical (ellipsoid-like) shape of the globular protein or due to the specific arrangement of hydrophilic sites on the lysozyme surface. If the first factor is dominant, then the difference in L_{max} could be used to separate spanning and nonspanning water clusters in computer simulations of hydrated globular proteins. The effect of the particular shape of a protein molecule on the distribution $P(L_{max})$ deserves further studies.

The radius of gyration R_g of the largest water cluster was analyzed in a similar way as to its maximum extension L_{max}. Figure 7 shows a pronounced two-peak structure of the probability distribution $P(R_g)$ of the radius of gyration over a wide range of hydration levels. This could mean that spanning and nonspanning networks are characterized by very different values of R_g. To check this possibility, we calculated the joint probability distribution $P(R_g,S_{max})$ of the radius of gyration R_g and the size of the largest cluster S_{max}, which is shown in

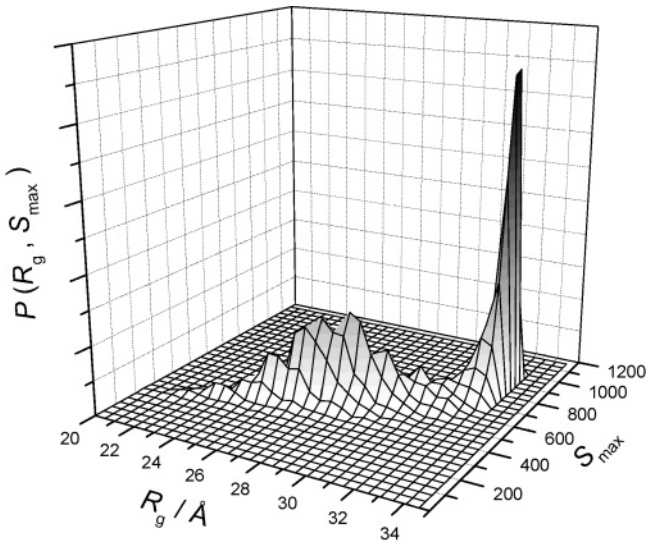

Figure 8. Joint probability distributions $P(R_g,S_{max})$ of the radius of gyration R_g and size S_{max} of the largest water cluster at the spherical surface of radius $R_{sp} = 30$ Å at $T = 425$ K and hydration level $C_1 \approx 0.088$ Å^{-2} ($N_w = 1200$).

Figure 8 for a sphere of radius $R_{sp} = 30$ Å and the threshold hydration level C_1. Indeed, the sharp peak of $P(R_g,S_{max})$ at large S_{max} values shows that the radius of gyration of a spanning cluster is close to the effective radius of a sphere ($R_{sp} + 3$ Å). The low and wide peak, positioned at a smaller S_{max} value in

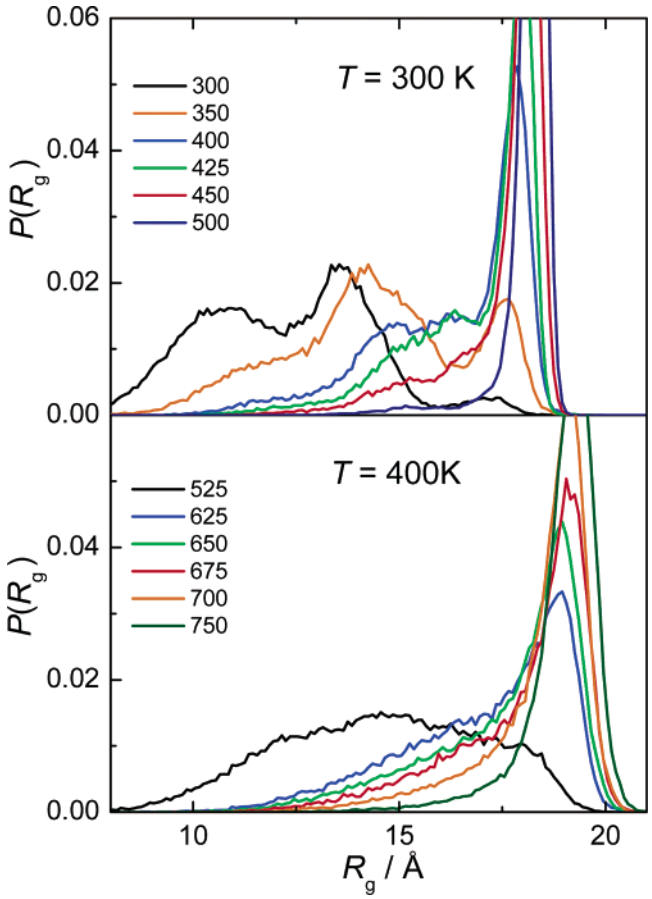

Figure 9. Probability distributions $P(R_g)$ of the radius of gyration R_g of the largest water cluster on the surface of lysozyme at two temperatures and various hydration levels. (N_w is given in the inset.) The blue and red lines approximately correspond to the surface coverages C_1 and C_2, respectively.

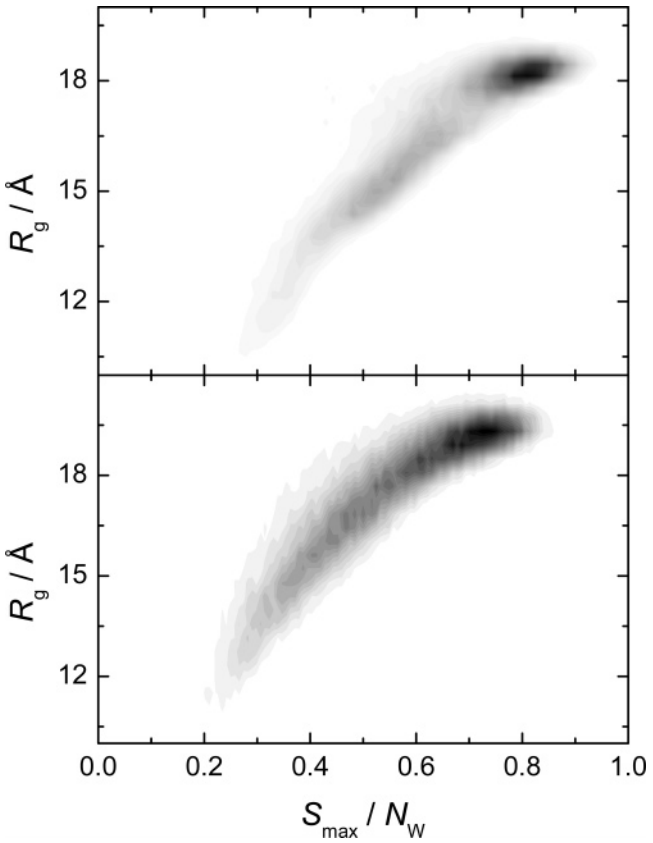

Figure 10. Projection of the joint probability distribution $P(R_g,S_{max})$ of the radius of gyration R_g and size S_{max} of the largest water cluster at the surfaces of lysozyme at the threshold surface coverage C_1 at T = 300 K (upper panel, N_w = 400) and T = 400 K (lower panel, N_w = 625). Shading is proportional to probability density. Each panel has its own (proper) probability scale.

Figure 8, corresponds to nonspanning clusters. Figure 7 indicates that R_g of the spanning clusters is not sensitive to the hydration level, whereas R_g of the nonspanning largest clusters continuously increases with increasing hydration level.

The behavior of the radius of gyration R_g of the largest water cluster on the surface of lysozyme is quite similar to that observed on the surfaces smooth hydrophilic spheres. The change in the probability distribution $P(R_g)$ of the radius of gyration of the largest cluster on the surface of lysozyme with increasing hydration level is shown in Figure 9. The correlation between the radius of gyration R_g and the size of the largest cluster S_{max} could be analyzed using the joint probability distribution $P(R_g,S_{max})$ (Figure 10). This correlation allows us to consider separately the radius of gyration for spanning and nonspanning clusters. The average value of R_g of the nonspanning largest cluster continuously increases with the hydration level (Figure 9). R_g of the spanning water cluster is practically independent of the hydration level and close to $R_g \approx 18$ Å at T = 300 K and $R_g \approx 19$ Å at T = 400 K (Figures 9 and 10). Such universality makes the radius of gyration the appropriate indicator of the spanning character of the largest water cluster.

The radius of gyration of the simulated model lysozyme is about 14 Å. For a homogeneous sphere of radius R, the radius of gyration is given by $R_g = \sqrt{3/5}R$. Thus, for a spherical lysozyme molecule with a uniformly distributed mass, the radius should be about 18 Å. The system of homogeneously distributed water molecules on the smooth surface of a sphere with such a radius should have a radius of gyration of $R_g \approx 18$ Å + 3 Å = 21 Å (see Figure 7 and its discussion above). The obtained lower values of R_g for the spanning water network at the lysozyme surface are obviously due to the nonspherical shape of the lysozyme molecule and the inhomogeneous distribution of water at the lysozyme surface. The latter factor originates from a irregular distribution of hydrophilic residues, which form the preferential sites for adsorption of water molecules at the surfaces of proteins.

At low hydration levels, we observe a splitting of the first peak of $P(R_g)$, corresponding to nonspanning water networks (Figure 9, T = 300 K). This splitting correlates with a similar behavior of the size distribution of the largest cluster $P(S_{max})$ at low hydration levels (Figure 12 in ref 34) and obviously reflects a preferential hydration of two comparatively large hydrophilic parts of the lysozyme surface.[2] The importance of the particular structure of the protein surface for various properties of the largest water cluster vanishes with increasing temperature (Figure 9, T = 400 K).

The probability distribution of the distance H_{max} from the center of mass of the largest water cluster to the center of a sphere also shows a two-peak structure over a wide range of hydration levels (Figure 11). Water clusters, covering the spherical surface completely or homogeneously, are represented by the sharp peak of $P(H_{max})$ at small values of $H_{max}/(R_{sp}$ + 3 Å) (left peaks in Figure 11). The second peak, positioned at higher values of $H_{max}/(R_{sp}$ + 3 Å), obviously represents the nonspanning largest clusters. With a decrease in water coverage, the right peak moves toward $H_{max}/(R_{sp}$ + 3 Å) = 1, which reflects increasing localization of the largest cluster within a small surface area.

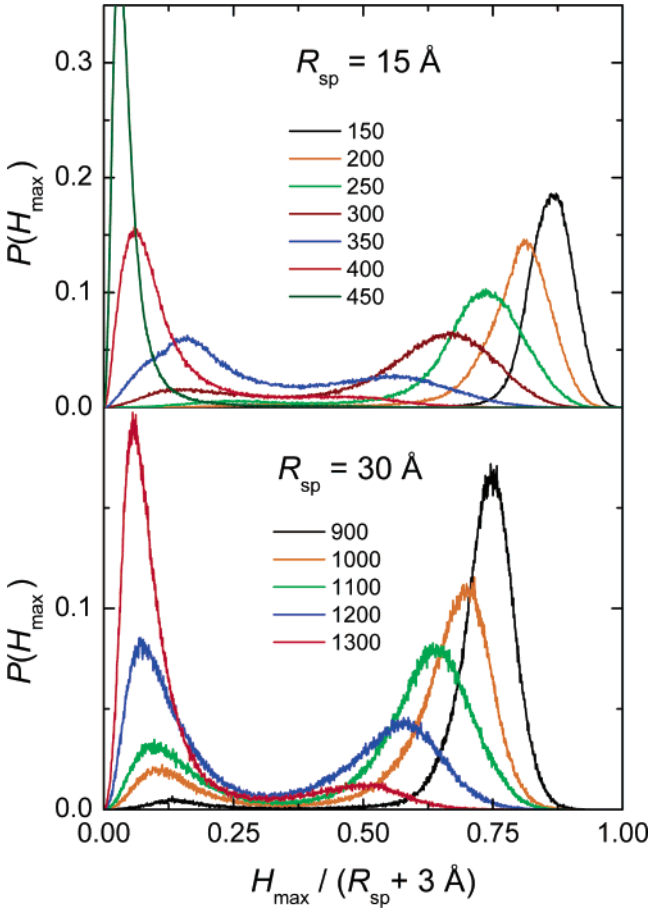

Figure 11. Probability distribution $P(H_{max})$ of the distance H_{max} between the center of mass of the largest cluster and the center of the sphere of radius $R_{sp} = 15$ and 30 Å at $T = 425$ K and various hydration levels. (N_w is given in the inset.) Blue and red lines approximately correspond to the threshold surface coverages C_1 and C_2, respectively.

For all spheres studied, a clear minimum of $P(H_{max})$ is observed near $H_{max} \approx 0.3$ ($R_{sp} + 3$ Å). Note that the center of mass of a surface spherical segment of height h is located at the distance $R_{sp} - h/2$ from the center. Therefore, the center of mass of an infinitely thin empty hemisphere is at the distance $H_{max} \approx R_{sp}/2$. If water covers homogeneously a hemisphere, then the center of mass of the water molecules should be at ($R_{sp} + 3$ Å)/2 from the center of the sphere. So, the distributions $P(H_{max})$ at all surface coverages (Figure 11) show a low probability of the largest clusters to cover homogeneously the hemisphere and slightly larger areas. This fact could be treated as an instability of the largest clusters of such sizes. On the spherical surface of a radius $R_{sp} = 30$ Å, a small peak in the probability distribution $P(H_{max})$ located at $H_{max} \leq 0.1$ ($R_{sp} + 3$ Å) appears already at the surface coverage $C \approx 0.066$ Å^{-2} (Figure 11, lower panel, black line), which is noticeably below the percolation threshold $C_1 = 0.088$ Å^{-2} (which corresponds roughly to the blue line). This observation shows that any spanning cluster spans essentially more than half of the spherical surface. Obviously, the small largest clusters must be strongly ramified to span such a large area.

The joint probability distribution $P(H_{max},S_{max})$ of the distance H_{max} and the size of the largest cluster S_{max} at the threshold hydration level C_1 are shown in Figure 12 for a sphere of radius $R_{sp} = 30$ Å. Two sharp peaks, separated by a deep well, show that the calculation of the distance H_{max} is an appropriate parameter to be used for the detection of spanning clusters on the surface of a finite object.

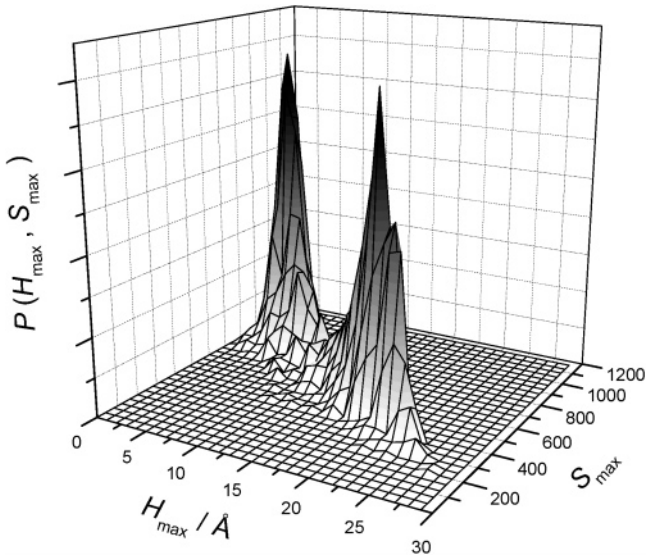

Figure 12. Joint probability distributions $P(H_{max},S_{max})$ of the distance H_{max} and size S_{max} of the largest cluster at a spherical surface of radius $R_{sp} = 30$ Å at $T = 425$ K and hydration level $C_1 \approx 0.088$ Å^{-2} ($N_w = 1200$).

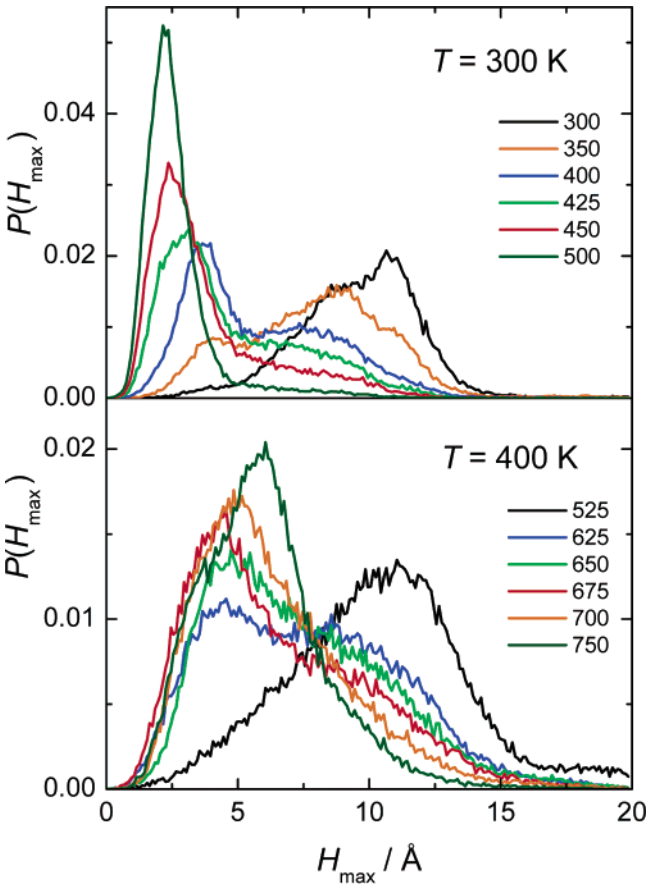

Figure 13. Probability distributions $P(H_{max})$ of the distance H_{max} between the center of mass of lysozyme and the center of mass of the largest water cluster at the surface of lysozyme at two temperatures and various hydration levels. (N_w is given in the inset.) The blue and red lines approximately correspond to the threshold surface coverages C_1 and C_2, respectively.

The probability distributions $P(H_{max})$ of H_{max} calculated for the largest water cluster on the surface of a lysozyme molecule at various hydration levels are shown in Figure 13. The evolution of $P(H_{max})$ with increasing hydration level reflects the existence of the two states of the largest clusters. The shallow minimum

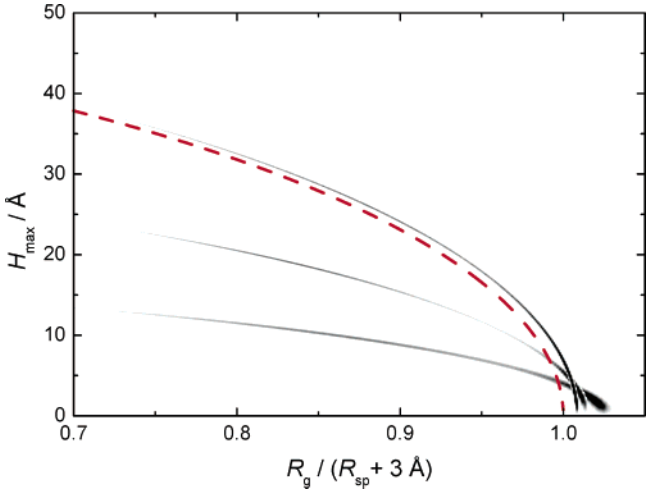

Figure 14. Correlation between the distance H_{max} and radius of gyration R_g of the largest water cluster at spherical surfaces obtained from the joint probability distribution $P(H_{max},R_g)$. The radii of the spherical surfaces R_{sp} = 15, 30, and 50 Å increase from the bottom to the top. The red dashed line shows the dependence $R_g(H_{max})$ as obtained from eq 4 for a sphere of R_{sp} = 50 Å. The hydration levels approximately correspond to the threshold surface coverages C_1 in each system studied. Shading is proportional to probability density.

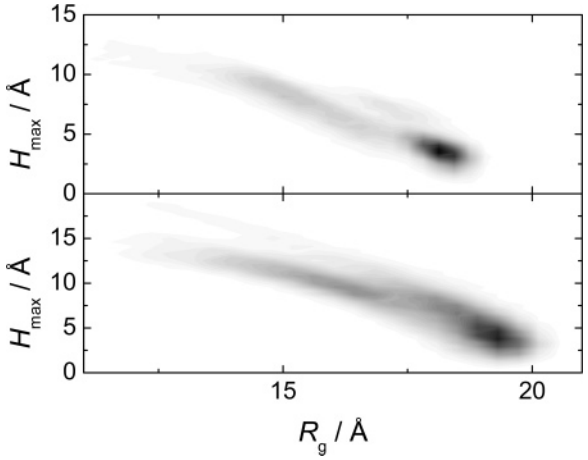

Figure 15. Joint probability distribution $P(H_{max},R_g)$ of the distance H_{max} and radius of gyration R_g of the largest water cluster at the surface of lysozyme at the threshold surface coverage C_1 at T = 300 K (upper panel, N_w = 400) and T = 400 K (lower panel, N_w = 625). Shading is proportional to probability density. Each panel has its own (proper) probability scale.

of $P(H_{max})$ between two states at about 6 Å at 300 K transforms into an isosbestic-like point at 400 K (Figure 13). This behavior differs from that observed for smooth spheres where two peaks are separated much more clearly (Figure 11). Obviously, the more complex shape of the lysozyme molecule and the chemical heterogeneity of its surface smears out the two-peak structure of $P(H_{max})$. The most probable value of H_{max} for spanning clusters at the lysozyme surface is about 3 Å at T = 300 K and about 5 Å at T = 400 K. The minimum of $P(H_{max})$ corresponds to the most unstable largest clusters. The value of H_{max} at the minimum could serve as a boundary between spanning and nonspanning clusters, which is about 6 and 7.5 Å at T = 300 and 400 K, respectively. These values are in good agreement with the results for clusters at spherical surfaces. Indeed, if we replace the lysozyme molecule by an effective sphere of radius 18 Å (see above), then we may expect the minimum of $P(H_{max})$ to occur at $H_{max} \approx 0.3\ (18 + 3)$ Å ≈ 6.3 Å.

Finally, we analyze the correlations between the two most significant properties, R_g and H_{max} of the largest water cluster, which could be used as sensitive indicators of the presence of a spanning water network. Correlations between H_{max} and R_g obtained from the calculation of the joint probability distribution $P(H_{max},R_g)$ for the three studied spherical surfaces are shown in Figure 14. Little scatter of the data points around a parabolic-like dependence R_g on H_{max} indicates a strong correlation of these two parameters. R_g and H_{max}, defined by eqs 1 and 2, respectively, are related to each other by the following equation

$$R_g^2 = \frac{\Sigma\, \vec{\mathbf{r}}_i^{\,2}}{N_w} - H_{max}^2 \qquad (3)$$

If all N_w molecules are at the same distance R_{sp} + 3 Å from the center of a sphere, $|\vec{\mathbf{r}}_i^{\,2}|$ is simply equal to $N_w(R_{sp} + 3\ \text{Å})^2$, i.e.

$$R_g = \sqrt{(R_{sp} + 3\ \text{Å})^2 - H_{max}^{\,2}} \qquad (4)$$

In the case of small H_{max} values, corresponding to spanning clusters, the dependence $R_g(H_{max})$ described by eq 4 is close to parabolic; for large H_{max} values (nonspanning largest clusters), it approaches a linear dependence. The eq 4 for a spherical surface of radius R_{sp} = 50 Å is shown by a dashed line in Figure 14. Deviations of the calculated correlation between R_g and H_{max} from eq 4 can be attributed to the fact that some water molecules in the largest cluster are out of the first water monolayer. The latter effect is especially pronounced in the case of a large spanning cluster (H_{max} close to zero).

The correlation between H_{max} and R_g of the largest water cluster at the surface of the lysozyme molecule, obtained from the calculation of the joint probability distribution $P(H_{max},R_g)$, is shown in Figure 15. In general, this correlation looks qualitatively similar to the case of water at the spherical surface; H_{max} decreases when the radius of gyration increases. The spanning and nonspanning largest clusters can be clearly separated at both temperatures. However, the spanning and nonspanning clusters obviously show different correlations between H_{max} and R_g This reflects the nonspherical shape of the lysozyme molecule and the inhomogeneity of its surface. Hence, contrary to an ideal spherical surface, H_{max} and R_g are not as closely related in the case of protein molecules.

Additionally, we have analyzed the lifetime of the spanning water networks at the surface of lysozyme at various hydration levels. The two-peak probability distribution of the largest cluster size was used to distinguish between spanning and nonspanning clusters (Figure 1 in this paper and Figure 12 in ref 34). In particular, at T = 300 K the largest cluster, which includes more than 270 molecules, was considered as a spanning one. Every 100th MD step (0.2 ps) we checked for the presence of a spanning cluster. The time t between the appearance and disappearance of a spanning cluster was defined as the product of the time step 0.2 ps and the number of consecutive configurations when the cluster remains spanning. The number $h(t)$ of spanning clusters, which have a lifetime t, allows us to calculate the number $N(t)$ of spanning networks living for a time t or longer[39]

$$N(t) = \sum_{t'=t}^{t'=\infty} h(t') \qquad (5)$$

The value $N(0)$ of the decay function $N(t)$ corresponds to the total number of spanning networks observed in the simulation run, i.e., the number of spanning networks that live during one

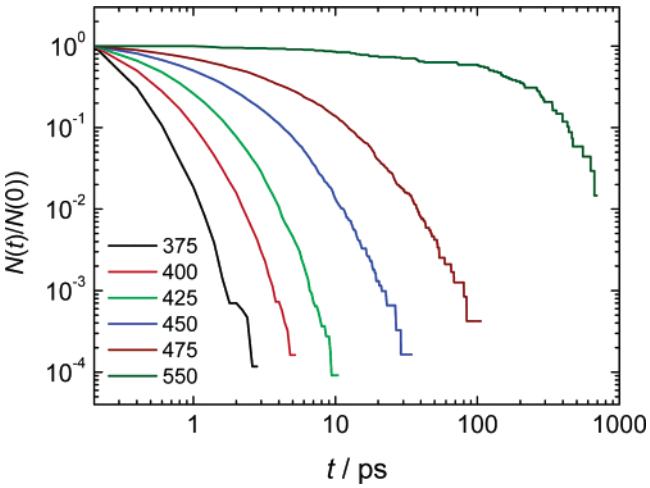

Figure 16. Decay function $N(t)/N(0)$ of the lifetime of a spanning water network at the surface of lysozyme at $T = 300$ K and various hydration levels. (N_w is given in the inset.) The blue and red lines approximately correspond to the threshold surface coverages C_1 and C_2, respectively.

TABLE 1: Parameters τ_{st} and α for Lysozyme at 300 K Computed by Fitting of $N(t)/N(0)$ with a Stretched Exponential Function (Eq 6)[a]

N_w	α	τ_{st}/ps	$\langle\tau_{st}\rangle$/ps	$\langle\tau\rangle$/ps	$\langle\tau_{HB}\rangle$/ps
375	0.857	0.202	0.219	0.197	1.088
400 ($\approx C_1$)	0.835	0.371	0.408	0.355	1.084
425	0.800	0.613	0.695	0.653	1.077
450 ($\approx C_2$)	0.633	1.038	1.462	1.164	1.075
475	0.573	2.648	4.524	4.727	1.072
550	(1)	184	184	176	1.059

[a] The lifetime of a single hydrogen bond $\langle\tau_{HB}\rangle$, calculated by eq 8, and the lifetimes of a spanning water network $\langle\tau_{st}\rangle$ and $\langle\tau\rangle$, calculated by eqs 7 and 8, respectively, are also given.

analyzed configuration at least. The simulated function $N(t)/N(0)$ of spanning water networks at the surface of lysozyme is shown in Figure 16 for various hydration levels.

At $t \geq 1$ ps, the function $N(t)/N(0)$ can be well fitted to a stretched exponential function

$$N(t)/N(0) = \exp\left(-\left(\frac{t}{\tau_{st}}\right)^{\alpha}\right) \quad (6)$$

where τ_{st} is a characteristic time and α is a stretching parameter. The deviation of the stretching parameter α from 1 is a signature of the nonexponential behavior of $N(t)/N(0)$. To take all data points equally into account at all time scales, we fitted the data to eq 6 in a logarithmic form. The obtained fitting parameters τ_{st} and α are listed in Table 1. The average lifetimes $\langle\tau_{st}\rangle$, calculated at various hydration levels by the equation

$$\langle\tau_{st}\rangle = \frac{\tau_{st}}{\alpha}\Gamma\left(\frac{1}{\alpha}\right) \quad (7)$$

with Γ as the gamma function, are given in Table 1.

The average lifetime $\langle\tau\rangle$ of a spanning water network can also be calculated directly, i.e., without any assumptions concerning the behavior of $N(t)/N(0)$

$$\langle\tau\rangle = N(0)^{-1}\int_0^{\infty} N(t')\,dt' \quad (8)$$

There is a good agreement between the average lifetimes of the spanning water networks, obtained in these two different ways (compare $\langle\tau\rangle$ and $\langle\tau_{st}\rangle$ in Table 1). This shows a stretched exponential decay of the spanning water clusters with time at all hydration levels. The deviation from the exponential decay increases with the hydration level and seems to achieve a maximum ($\alpha \approx 0.6$) at the percolation threshold, indicating the existence of a broad range of time scales. Far above the percolation threshold, the decay function $N(t)$ of the spanning water network could not be fitted satisfactorily to eq 6. As a result, the quality of the fit for $N_w = 550$ is worse compared to the quality of the fits at the other hydration levels given in Table 1.

It is reasonable to compare the lifetime of a spanning network with the average lifetime $\langle\tau_{HB}\rangle$ of a single water−water hydrogen bond. Various procedures can be used to calculate $\langle\tau_{HB}\rangle$ from MD simulations. In the present paper, we adopt a procedure similar to the one used to study the lifetime of a spanning water network. Namely, we calculate the number $N'(t)$ of water−water hydrogen bonds that occur and remain continuously unbroken during the time interval t or longer. The distribution $N'(t)$ and the average lifetime $\langle\tau_{HB}\rangle$ are found rather sensitive to the sampling frequency. In fact, the use of a long interval between sampled configurations assumes that the breaking and restoring of some hydrogen bonds at shorter time intervals are ignored. We have chosen the time interval between the analyzed configurations to be equal to 0.2 ps, i.e., exactly the same as used in the analysis of the lifetime of a spanning water network. The average lifetimes $\langle\tau_{HB}\rangle$ of water−water hydrogen bonds near the lysozyme surface at various hydration levels are shown in Table 1. Note that $\langle\tau_{HB}\rangle$ calculated for hydration water at the lysozyme surface is slightly higher than the value $\langle\tau_{HB}\rangle \approx 0.9$ ps obtained by applying the same procedure for the bulk liquid water at ambient conditions. The latter value is in good agreement with the average water−water hydrogen bond lifetime, obtained in bulk water using the same sampling frequency 0.2 ps.[42]

4. Conclusions

The formation of a quasi-two-dimensional spanning water network at the surface of a single protein molecule can be identified with the first appearance of a water monolayer, which is a necessary condition for completely restoring the internal dynamics of proteins, i.e., the dynamics observed in the case of full hydration. Besides, even in the latter case (protein in aqueous solution), the spanning network of surface water can break with temperature and pressure or due to the addition of cosolvents. This may have important consequences for the protein structure, dynamics, and hence its function. Therefore the properties of spanning networks of hydration water on the surfaces of proteins should be studied in detail, in particular, by computer simulations.

Percolation theory does not predict how a percolating (spanning) network should appear and how it can be detected and characterized in such closed systems as the surface of a finite object. In a previous paper,[34] we have shown how the formation of a spanning water network occurs at the surface of a protein molecule. In the present paper, we performed computer simulation studies of the various properties of spanning and nonspanning water networks at the simplest closed surface, namely, smooth hydrophilic spherical surfaces, and extend this analysis to the surface of a real protein, a lysozyme molecule.

The two-peak structure of the probability distribution $P(S_{max})$ of the largest cluster size reflects the two different contributions from the largest nonspanning and spanning clusters, respectively.[34] This property allows us to identify the spanning character of the largest cluster based on its size. To explore the

specificity of various topological properties of a spanning water network, we studied their mutual correlations and correlations with the size S_{max} of the largest cluster.

We have found that in the case of a sphere the maximum linear extension L_{max} of the largest cluster achieves values exceeding the diameter of the sphere, even for comparatively small nonspanning clusters. The nonspherical shape of the lysozyme molecule seems to increase the difference between the values of L_{max} for spanning and nonspanning clusters. However, we cannot exclude the existence of two kinds of spanning clusters that envelop the ellipsoid-like lysozyme molecule in two different ways, along the major or along the minor axis of the ellipsoid.

The distance H_{max} from the center of mass of the largest water cluster to the center of the sphere and the radius of gyration of the largest cluster R_g are the topological parameters of the network, which directly reflect its spanning or nonspanning character. H_{max} is close to zero for all spanning clusters, whereas for the majority of nonspanning clusters, $H_{max} > 0.5R_{sp}$. A deep minimum in the probability distribution $P(H_{max})$ indicates an instability of the largest clusters that span roughly half of the spherical surface. In the case of a sphere, all spanning clusters have a radius of gyration R_g close to the radius of a sphere R_{sp} (more correctly, $R_g \approx R_{sp} + 3$ Å for water near smooth hydrophilic spheres).

The behavior of H_{max} and R_g of the largest water cluster on the surface of the lysozyme molecule does not allow for such a clear geometrical interpretation as in the case of an ideal sphere with smooth (structureless) surface. Due to the complex shape and heterogeneous chemical structure of a protein surface, water molecules are distributed inhomogeneously in the hydration shell. Besides, properties of water molecules noticeably depend on their location on the protein surface. Obviously, these factors essentially affect the structural properties of the nonspanning (local) water networks at low hydration levels and low temperatures. Properties of the spanning water network seem to be much more universal. In particular, the radius of gyration of any spanning water cluster should exceed at least the radius of gyration of the lysozyme molecule and approach the effective radius of the completed first hydration shell. This allows us to use both H_{max} and R_g to distinguish spanning and nonspanning clusters of water at the surface of the protein molecule.

The average lifetime of a spanning water network strongly depends on the hydration level, whereas the lifetime of a single hydrogen bond is about 1 ps over a wide range of hydration levels (Table 1). At the percolation threshold, the lifetime $\langle\tau\rangle$ of a spanning network is comparable to the lifetime of a single water−water hydrogen bond. This indicates that each water molecule of a largest cluster breaks and creates on the average one hydrogen bond before this cluster changes its character from spanning to nonspanning or vice versa. We note that the lifetime $\langle\tau\rangle$ of a spanning water network near the percolation threshold is significantly smaller than the residence time of water molecules at the lysozyme surface in solution.[43]

Some internal protein movements could be affected (or even activated) by the spanning water network, when their characteristic time scales become comparable with the lifetime of the spanning water network, which represents an example of the slaving effect mentioned in the Introduction. For example, the collective dynamics of polypeptide side chains of lysozyme are described by characteristic times of ~4 ps.[44] Such motions could be influenced/activated by a spanning water network just above the percolation threshold (Table 1). Indeed, such protein dynamics are not observed in dry proteins.[45]

Hence, the presence of a spanning network of water molecules, connected via relatively strong (stable) and flexible hydrogen bonds, could have specific effects on the dynamic properties of the protein + water system. Besides the appearance of the eigenmodes of such networks,[46] the "rubberlike" character of a spanning water network may not only facilitate the dynamics of various movements of the protein molecule but may also lead to their coupling. Studies of various dynamic properties of hydrated proteins with and without spanning networks of hydration water should be carried out to elucidate their roles in protein dynamics and function.

Acknowledgment. We thank the Deutsche Forschungsgemeinschaft (DFG-Forschergruppe 436) for financial support.

References and Notes

(1) Kuntz, I. D., Jr.; Kauzmann, W. *Adv. Protein, Chem.* **1974**, *28*, 239.
(2) Rupley, J. A.; Careri, G. *Adv. Protein Chem.* **1991**, *41*, 37.
(3) Teeter, M. M. *Annu. Rev. Biophys. Chem.* **1991**, *20*, 577.
(4) Teeter, M. M. *Proc. Natl. Acad. Sci. U.S.A.* **1984**, *81*, 6014.
(5) Makarov, V. A.; Andrews, B. K.; Smith P. E.; Pettitt B. M. *Biophys. J.* **2000**, *79*, 2966.
(6) Teeter, M. M.; Yamano, A.; Stec, B.; Mohanty, U. *Proc. Natl. Acad. Sci. U.S.A.* **2001**, *98*, 11242.
(7) Dorbez-Sridi, R.; Cortez, R.; Mayer, E.; Pin, S. *J. Chem. Phys.* **2002**, *116*, 7269.
(8) Nakasako, M. *J. Biol. Phys.* **2002**, *28*, 129.
(9) Head-Gordon, T.; Sorenson, J. M.; Pertsemlidis, A.; Glaeser, R. M. *Biophys. J.* **1977**, *73*, 2106.
(10) Cheng, Y.-K.; Rossky, P. *Nature* **1998**, *392*, 696.
(11) Smolin, N.; Winter, R. *J. Phys. Chem. B* **2004**, *108*, 15928.
(12) Karvounis, G.; Nerukh, D.; Glen, R. C. *J. Chem. Phys.* **2004**, *121*, 4925.
(13) Tarek, M.; Tobias, D. J. *Biophys. J.* **2000**, *79*, 3244.
(14) Dellerue, S. Bellissent-Funel, M.-C. *Chem. Phys.* **2000**, *258*, 315.
(15) Bizzarri, A. R.; Cannistraro, S. *J. Phys. Chem. B* **2002**, *106*, 6617.
(16) Russo, D.; Hura, G.; Head-Gordon, T. *Biophys. J.* **2004**, *86*, 1852.
(17) Halle, B. *Philos. Trans. R. Soc. London, Ser. B* **2004**, *359*, 1207.
(18) Pal, S. K.; Zewail A. H. *Chem. Rev.* **2004**, *104*, 2099.
(19) Brooks, C. L., III; Karplus, M. *J. Mol. Biol.* **1989**, *208*, 159.
(20) Steinbach, P. J.; Loncharich, R. J.; Brooks, B. R. *Chem. Phys*. **1991**, *158*, 383.
(21) Steinbach, P. J.; Brooks, B. R. *Proc. Natl. Acad. Sci. U.S.A.* **1993**, *90*, 9135.
(22) Wang, C. X.; Bizzarri, A. R.; Xu, Y. W.; Cannistraro, S. *Chem. Phys.* **1994**, *183*, 155.
(23) Bizzarri, A. R.; Wang, C. X.; Chen, W. Z.; Cannistraro, S. *Chem. Phys.* **1995**, *201*, 463.
(24) Phillips, G. N., Jr.; Pettitt, B. M. *Protein Sci.* **1995**, *4*, 149.
(25) Careri, G.; Giansanti, A.; Rupley, J. A. *Proc. Natl. Acad. Sci. U.S.A.* **1986**, *83*, 6810.
(26) Careri, G.; Giansanti, A.; Rupley, J. A. *Phys. Rev. A* **1988**, *37*, 2703.
(27) Rupley, J. A.; Siemankowski, L.; Careri, G.; Bruni, F. *Proc. Natl. Acad. Sci. U.S.A.* **1988**, *85*, 9022.
(28) Bruni, F.; Careri, G.; Leopold, A. C. *Phys. Rev. A* **1989**, *40*, 2803.
(29) Sokolowska, D.; Krol-Otwinowska, A.; Moscicki, J. K. *Phys. Rev. E* **2004**, *70*, 052901.
(30) Smith, J. C.; Merzel, F.; Bondar, A.-N.; Tournier, A.; Fischer, S. *Philos. Trans. R. Soc. London, Ser. B* **2004**, *359*, 1181.
(31) Daniel, R.M.; Finney, J. L.; Réat, V.; Dunn, R.; Ferrand, M.; Smith, J. C. *Biophys. J.* **1999**, *77*, 2184.
(32) Turnier, A. L.; Xu, J.; Smith, J. C. *Biophys. J.* **2003**, *85*, 1871.
(33) Fenimore, P. W.; Frauenfelder, H.; McMahon, B. H.; Parak, F. G. *Proc. Natl. Acad. Sci. U.S.A.* **2002**, *99*, 16047.
(34) Oleinikova, A.; Smolin, N.; Brovchenko, I.; Geiger, A.; Winter, R. *J. Phys. Chem. B* **2005**, *109*, 1988.
(35) Kundrot, C. E.; Richards, F. M. *J. Mol. Biol.* **1987**, *193*, 157.
(36) Cornell, W. D.; Cieplak, P.; Bayly, C. I.; Gould, I. R.; Merz, K. M., Jr.; Ferguson, D. M.; Spellmeyer, D. C.; Fox, T.; Caldwell, J. W.; Kollman, P. A. *J. Am. Chem. Soc.* **1995**, *117*, 5179.
(37) Jorgensen W. L.; Chandrasekhar, J.; Madura, J. D.; Impey, R. W.; Klein, M. L. *J. Chem. Phys.* **1982**, *77*, 926.
(38) Brovchenko, I.; Geiger, A.; Oleinikova, A. *J. Chem. Phys.* **2004**, *120*, 1958.

(39) Geiger, A.; Mausbach, P.; Schnitker, J.; Blumberg, R. L.; Stanley, H. E. *J. Phys.* **1984**, *45*, C7−13.

(40) Brovchenko, I.; Oleinikova, A. Molecular organization of gases and liquids at solid surfaces. In *Handbook of Theoretical and Computational Nanotechnology*; Rieth, M., Schommers, W., Eds.; American Scientific Publishers: Stevenson Ranch, CA, 2005, in press.

(41) Brovchenko, I.; Geiger, A.; Oleinikova, A. In *New Kinds of Phase Transitions: Transformations in Disordered Substances*; Brazshkin, V. V., Buldyrev, S. W., Ryshov, V. N., Stanley, H. E., Eds.; Kluwer Academic Publishers: Norwell, MA, 2002; p 367.

(42) Zou, Q.; Bennion, B. J.; Daggett, V.; Murthy, K. P. *J. Am. Chem. Soc.* **2002**, *124*, 1192.

(43) Marchi, M.; Sterpone, F.; Ceccarelli, M. *J. Am. Chem. Soc*. **2002**, *124*, 6787.

(44) De Francesco, A.; Marconi, M.; Cinelli, S.; Onori, G.; Paciaroni, A. *Biophys. J.* **2004**, *86*, 480.

(45) Fitter, J.; Lechner, R. E.; Büldt, G.; Dencher, N. A. *Proc. Natl. Acad. Sci. U.S.A.* **1996**, *93*, 7600.

(46) Pal, S.; Balasubramanian, S.; Bagchi, B. *J. Chem. Phys.* **2004**, *120*, 1912.